JOURNAL OF AGRICULTURAL AND FOOD CHEMISTRY

Thermo-FTIR Spectroscopic Study of the Siderophore Ferrioxamine B: Spectral Analysis and Stereochemical Implications of Iron Chelation, pH, and Temperature

HAGAR SIEBNER-FREIBACH,[†] SHMUEL YARIV,[#] YITZHAK LAPIDES,[#] YITZHAK HADAR,[§] AND YONA CHEN*,[†]

Department of Soil and Water Sciences and Department of Microbiology and Plant Pathology, Faculty of Agricultural, Food and Environmental Quality Sciences, The Hebrew University of Jerusalem, P.O. Box 12, Rehovot 76100, Israel, and Department of Inorganic Chemistry, The Hebrew University of Jerusalem, Jerusalem 91904, Israel

FTIR spectra of the microbial siderophore, ferrioxamine B, and its nonchelated form (iron free; desferrioxamine B) were studied to facilitate in-depth investigation on the undisrupted structure of the siderophore and its interactions with the environment. Effects of iron chelation as well as those of various levels of pH and temperature on the stereochemical structure of the free ligand and the ferric complex were examined. The presence of a number of functional groups in these compounds and the mutual interaction between them resulted in significant shifts and overlapping of their characteristic absorption bands. Thermal and pH treatments combined with a comprehensive use of curve-fitting analysis facilitated bands resolution. Absorption bands of all functional groups were identified. The results imply that the compact and rigid structure of the ferric complex (ferrioxamine B) is sustained by intense and specific intramolecular hydrogen bonds. Dehydration was the main process observed at low temperature (25−60 °C). At 105 °C the free ligand form (desferrioxamine B) had already begun to decompose, whereas ferrioxamine B exhibited stability. The thermal destruction became acute at the 170 °C treatment for both molecules. The secondary amide groups and the hydroxamate groups, which comprise the binding site for the Fe atom in the complex, were found to be the most sensitive to the thermal degradation. Significant pH effects were observed only for desferrioxamine B samples at pH 9, accompanied by partial decomposition, similar to that observed at 105 °C. Deprotonation of desferrioxamine B was found to begin with the deprotonation of the NH_3^+ group. Characteristics of the rigid conformational structure of the ferric complex and the state of the NH_3^+ group, both assumed to play an important role in the recognition and uptake of the siderophore by membranal receptors, were elaborated by means of FTIR and are discussed in detail.

KEYWORDS: Desferrioxamine B; ferrioxamine B; IR spectroscopy; siderophore

INTRODUCTION

Iron deficiencies are common in large parts of the world, notwithstanding the abundance of this element in the earth's crust (*1*, *2*). Low solubility of iron minerals leads to a very low concentration in the solution of calcareous and aerated soils (*3*). To handle this shortage, microorganisms have developed a system based on secretion of siderophores. These low molecular weight chelates scavenge iron from the surroundings, and then they are efficiently absorbed by its producer as well as other microorganisms (*4*). Various studies have demonstrated improvement in iron nutrition of plants when siderophores were used as an iron source (*5*−*9*). The microbial siderophore ferrioxamine B belongs to the important group of hydroxamate siderophores (*4*). We chose this compound due to its high stability constant with iron over a wide range of pH values (*11*) and its stability against microbial degradation. This siderophore is produced by soil microorganisms, *Streptomyces* and *Nocardia* (*10*), and was found to be useful in supplying plants with iron. The activity of ferrioxamine B has been extensively studied in different fields of science including medical research.

The desferric molecule (**Figure 1A**) is a hexadentate ligand consisting of three bidentate hydroxamic groups. The residual chain includes two secondary amide groups and an aliphatic chain. The saturated amine group on one edge of the linear molecule gives the molecule a positive charge in acid to slightly

* Corresponding author (telephone +972-8-9489234; fax +972-8-9468565; e-mail yonachen@agri.huji.ac.il).
[†] Department of Soil and Water Sciences, Hebrew University of Jerusalem, Rehovot, Israel.
[#] Department of Inorganic chemistry, Hebrew University of Jerusalem, Jerusalem, Israel.
[§] Department of Microbiology and Plant Pathology, Hebrew University of Jerusalem, Rehovot, Israel.

10.1021/jf048359k CCC: $30.25
Published on Web 04/02/2005

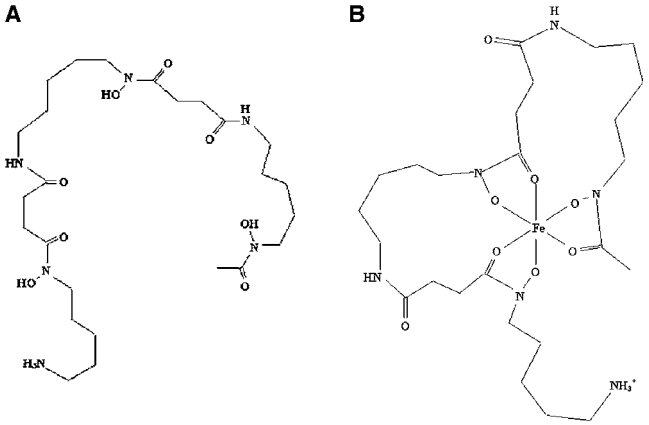

Figure 1. Schematic diagrams of (**A**) desferrioxamine B, the free ligand of the siderophore ferrioxamine B, and (**B**) ferrioxamine B, the ferric complex of desferrioxamine B.

alkaline solutions (*11*). Upon Fe^{3+} chelation, oxygen atoms of the hydroxamate groups bind to Fe (**Figure 1B**), the three hydroxyls are deprotonated, and three identical asymmetrical chelation rings are formed, creating a distorted octahedron centralized by Fe. The open chain, ending with the NH_3^+ group, has been found to point away from the Fe center (*12*). The iron complex (ferrioxamine B) obtains a wide and fairly flat configuration of 5.5 Å total thickness (*12*). In contrast with the linear open chain of the free ligand (desferrioxamine B), which exhibits exposed active sites, the ferric complex presents a rather hydrophobic face apart from the NH_3^+ group in the molecule edge.

Although X-ray crystallography of the ferric complex of ferrioxamine B (*12*) supplied crucial information about this molecule, the undisrupted structures of ferrioxamine B as well as desferrioxamine B, especially in natural environments, are important factors, and they are still hard to detect. FTIR spectroscopy is an easy and useful option that could be used for the characterization of siderophore condition and interactions with its environment (e.g., free ligand or iron complex; adsorbed to a solid phase or free in solution). An efficient use of this method requires a detailed analysis of the spectrum and peak assignment to the various functional groups. Only a few papers have dealt with the FTIR spectra of ferrioxamine B, but none of them provided a comprehensive interpretation of the spectra. Some of the studies provided a contradictory interpretation for the same band (*13, 14*). Others marked general ranges of absorption (*13*), which included several bands, and did not enable the interpretation of the reaction of the various functional groups under different environmental conditions, such as temperature and pH, and their interactions with other compounds.

Detailed studies that deal with hydroxamic acids (*15, 16*) and oximes (*17*) could serve as a reference for the hydroxamic groups. Still, the siderophore ferrioxamine B is much more complicated, and thus its FTIR spectra require special analysis. Mutual influences of the various functional groups significantly affect the frequency of characteristic bands. Also, a significant overlapping of absorption bands takes place, due to multiplicity of functional groups. To resolve this problem, we have employed an extensive work using a curve-fitting technique. The response of the various functional groups to different environmental conditions, as well as iron chelation, was examined in this study. Stereochemical implications and potential effects on the function of the siderophore are discussed. The interpretation of the FTIR spectra, which is exhibited in this study, is expected to be instrumental for the identification of the binding mechanism to solid phases or other organic compounds, which could have an important effect on the function and reactivity of the siderophore. These aspects are extremely important in soils where the siderophore most likely interacts with the solid phase. It could also be applicable to other fields of science, such as medicine, where this siderophore is used for human health care.

MATERIALS AND METHODS

The methylsulfonate salt of the desferric form of the microbial siderophore ferrioxamine B (desferrioxamine B) was purchased as the medical reagent Desferal from Ciba-Geigy Ltd. (Basel, Switzerland) and used in this study.

Desferrioxamine B was dissolved in distilled water. The complex with iron (ferrioxamine B) was prepared by adding $FeCl_3$ to the free ligand solution with a 10% excess of iron and then centrifuged at 106000*g* and filtered through 0.1 μm filters, to remove iron colloids.

Solutions of both desferrioxamine B and ferrioxamine B were prepared at four pH levels (4.0, 6.0, 7.5, and 9.0). The pH was adjusted with $HClO_4$ and KOH to the desired level, and then the volume was adjusted with distilled water to obtain a concentration of 1.0 mM. The solutions were gently freeze-dried, ground, and kept in a desiccator.

FTIR Spectra. Air-dried powders with KBr (for IR spectroscopy) at 25 °C were pressed into a disk and then reground gently and re-pressed. This procedure was applied to homogeneously scatter the examined substances in the disk. One hundred milligram disks composed of air-dried desferrioxamine B or ferrioxamine B (at pH values of 4.0, 6.0, 7.5, and 9.0), at various concentrations (0.5, 1.0, and 2.0 mg per disk) were prepared with KBr. The FTIR spectra were recorded using a Nicolet Magna-IR model 550. According to the results, optimal concentrations of 0.5 and 2 mg per disk for desferrioxamine B and ferrioxamine B, respectively, were determined.

Thermal Treatments. FTIR spectra were recorded following preparation at room temperature (25 °C), and the KBr disks were then gradually heated overnight to 60, 105, and 170 °C. The disks became opaque after the thermal treatments, and they were thus re-pressed, without regrinding, to restore transparency.

Curve-Fitting. Curve-fitting was performed on the FTIR spectra using the data processing software GRAMS/AI of Thermo Galactic. It uses the Levenberg−Marquardt algorithm when the gradient is far from the minimum, then switches to the Hessian matrix methods to determine the best possible solution when the algorithm reaches a minimum value of χ^2. Baseline corrections and analysis were performed over restricted ranges of the spectrum. Among existing methods used to analyze and describe the exact line shape of FTIR peaks, we selected the Lorentzian line shape, which is suitable for spectroscopic data analysis and provided highly satisfactory curve-fitted spectra.

The Savitzki−Golay smoothing algorithm, used in Root Mean Squared (RMS) noise estimation, takes into account the number of data points within the width of the smallest peak. Fitting a few sharp peaks in the presence of broad ones could result in an underestimation of the RMS noise, thus leading to artificially high levels of reduced χ^2, whereas the solution is actually very good. This is the case in the spectra of desferrioxamine B and ferrioxamine B (see, for example, **Figure 2**). Indeed, very high values of reduced χ^2 were received. To resolve this problem in the present study, the RMS was graphically estimated over a narrow examined range, manually operating this option in the program. A value 2 orders of magnitude lower was then manually inserted to avoid possible overestimation of the RMS noise. Solutions were accepted only when they converged, good and highly reproducible χ^2 values were obtained, and the results were compatible with the known chemical composition of the molecule.

RESULTS

An example of the curve-fitting results, the spectrum of desferrioxamine B at 25 °C and pH 7.5 in the frequency range of 3500−2500 cm^{-1}, is presented in **Figure 2**. Data obtained at different pH values and thermal conditions and analyzed by

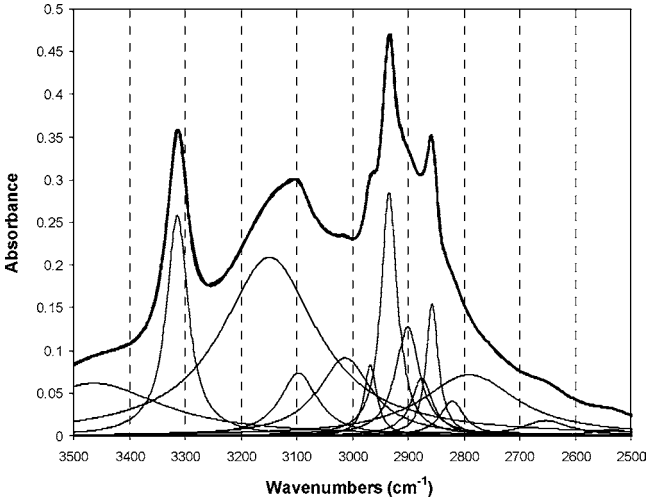

Figure 2. Curve-fitted spectrum of desferrioxamine B: the spectrum was recorded on KBr disks (25 °C, pH 7.5). Bold lines represent measured spectrum and fitted line, which are overlapping. Gray lines represent the spectra assembling the fitted line as it was analyzed using GRAMS/AI software produced by Thermo Galactic. Peak values and appropriate assignments are detailed in **Table 1**.

the curve-fitting technique are summarized for desferrioxamine B and ferrioxamine B spectra in **Tables 1** and **2**, respectively. The tables include band assignments, frequencies of maxima, relative band intensities, and band shapes.

Effects of Fe^{3+} Chelation. A comparison of the FTIR spectra of desferrioxamine B and ferrioxamine B (the iron complex) at 25 °C and pH 7.5 is presented in **Figure 3**.

The most conspicuous effect of the iron chelation on the spectra at the high-range frequencies is the appearance of a strong broad peak at 3443 cm^{-1} (**Figure 3A**). Curve-fitting analysis of this range in the ferrioxamine B spectrum revealed that it is composed of a few strong peaks (**Table 2**, bands at 3600−3350 cm^{-1}). The frequency of the band assigned to the N−H of the secondary amide decreased significantly from a sharp peak at 3313 cm^{-1} to a broad one at 3269 cm^{-1} upon iron chelation.

The broad, nonsymmetrical peak at 3101 cm^{-1} along with the shoulder at 3140 cm^{-1} (**Figure 3**) in the desferrioxamine B spectra did not appear in the ferrioxamine B spectra, in which a single peak at 3084 cm^{-1} was exhibited. The curve-fitting analysis of this range revealed a strong and broad O−H peak at 3149 cm^{-1} in the desferrioxamine B spectra (**Figure 2**; **Table 1**) that did not appear in those of ferrioxamine B, excluding a very weak and broad trace peak seen in the latter spectrum at 25 °C (**Table 2**). The C−NH overtone band of the secondary amide was shifted from 3096 to 3084 cm^{-1}. In a lower frequency range (3050−2800 cm^{-1}), a significant overlapping of the absorption bands of the aliphatic groups and those of NH_3^+ in the spectra of desferrioxamine B and ferrioxamine B was exhibited. Therefore, the use of the curve-fitting technique to study the effect of the different treatments on these groups was inevitable. The peak assigned to CH_3 at 2967 cm^{-1} in the desferrioxamine B spectrum shifted to 2951 cm^{-1} upon iron chelation (**Tables 1** and **2**; respectively). The frequency of the NH_3^+ symmetric stretching band increased significantly from 2901 to 2947 cm^{-1}, whereas the asymmetric stretching band remained unchanged.

An intensive overlapping of vibrations was also exhibited at the range of 1700−1550 cm^{-1}. We have assigned these bands to the amide I band (C═O stretching) of both the hydroxamate and the secondary amide groups, the amide II band (C−N−H coupling) of the latter, and the NH_3^+ group. The spectra of desferrioxamine B exhibited very strong absorption at 1624 cm^{-1} with a shoulder at 1650 cm^{-1} (**Figure 3B**). This strong peak shifted upon iron chelation to 1573 cm^{-1} in the ferrioxamine B spectrum and exposed the shoulder at 1650 cm^{-1}, which became an evident peak. The peak of medium intensity assigned to the amide II band (C−NH), which appeared at 1568 cm^{-1} in the desferrioxamine B spectrum, was hidden in the spectra of the ferrioxamine B by the strong peak of the hydroxamic C═O (**Figure 3B**).

Table 1. Absorption Bands of the Curve-Fitted Infrared Spectra of Desferrioxamine B[a]

band assignment	frequency (wavenumber, cm^{-1}) 25 °C	105 °C	pH 9
HOH stretch	3464 w, vbr		3540 vw, br
NH_2 stretch			3410 m, br
			3323 m, sp
N–H stretch secondary amide (hydrated)	3313 vs, sp	3317 s, sp	3309 m, sp
N–H stretch secondary amide (unhydrous)		3266 m, br	
O–H stretch	3149 s, br	3160 s, vbr	3139 vs, vbr
C–N–H overtone	3096 w	3090 m	3093 w
NH_3^+ stretch	3013 m	3015 m	3000 w, br
CH_3 as. stretch	2967 w, sp	2966 m, sp	2966 w, sp
CH_2 as. stretch	2933 vs, sp	2934 s, sp	2934 vs, sp
NH_3^+ sym stretch	2901 m	2902 s, br	2903 w
CH_3 sym stretch	2875 vw, sp	2868 w	2880 w
CH_2 sym stretch	2856 m, sp	2856 m, sp	2857 m, sp
NH_3^+ overtones and combination tones	2821 vw	2821 w, br	2820 w
	2790 m, vbr	2763	2734 m, br
	2652 w	2657	2626 m, br
	2535 w	2544	2554 w
			2488 w
			2430 w
			2393 w
			2285 w
products of decomposition			1732 w, vbr
	1697 vvw	1700 m	1699 s
			1671 m
C═O stretch (secondary amide)	1651 m	1649 s	1651 s
HOH deform	1634 s	1635 vw	1634 m
C═O stretch (hydroxamate)	1624 vs	1623 vs	1622 vs
NH_3^+ as. deform	1608 m, br	1605 vw, br	1607 vw
NH_2 in-plane deform			1596 w, br
C–N–H (secondary amide)	1571 m	1570 m	1569 m
C–N–H (secondary amide)	1564 m	1561 m	1561 w
NH_3^+ sym deform	1551 m,br	1547 m	1548 w, br
CH_2	1463 w, br		
CH_3	1461 m	1459 m	1461 w
C–H vibrations: exact	1453 w		1453 m, br
location derives from	1436 w	1437 w	1436 w
adjacency of different	1424 w	1425 w	1427 m
functional groups	1416 w	1416 w	1414 m
		1404 w	1406 w
O–H deform	1397 m	1397 w, sp	1397 s
CH_3	1373 w	1373 w	1372 m
C–N stretch N–H bend	1271	1271	1271
(secondary amide)[b]	1254	1254	1254
C–N stretch[b]	1181	1181	1181
	1163	1163	1163
	1134 w	1134 w	1134 w
N–O[b]			1009
	989	989	986
	964	964	964

[a] Relative band height (s, strong; m, medium; w, weak; v, very) and shape (sp, sharp; br, broad) are described. The shape of bands with an average broadness is not mentioned in the table. [b] These bands were determined without curve-fitting.

Table 2. Absorption Bands of the Curve-Fitted Infrared Spectra of Ferrioxamine B[a]

band assignment	frequency (wavenumber cm^{-1}) 25 °C	105 °C	pH 9
HOH stretch	3619		3617
	3587		3586
	3554		3555
	3518		3521
	3479		3482
	3435		3439
	3381		3384
N–H stretch (secondary amide)	3269 vs, br	3274 s, br	3272 vs, br
Traces	3159 vw, vbr		3159 vw, br
C–N–H overtone	3084 m	3071 s, br	3084 m
NH_3^+ as. stretch	3012 m	3013 w	3009 m
CH_3 as. stretch	2951 vw	2986 w	2951 vw
CH_2 as. stretch	2932 vs, sp	2933 vs,	2931 vs, sp
NH_3^+ sym stretch	2947 m, br	2939 m	2949 w br
CH_3 sym stretch	2872 w, sp	2871 w	2868 w
CH_2 sym. stretch	2858 m, sp	2859 m	2856 w, sp
NH_3^+ overtones and combination tones	2817 w	2815 m, br	2818 w
	2752 w	2745 w, br	2753 w
	2653 w;	2646 w, br	2651 w
	2550 w	2545 w, br	2543 w, br
product of decomposition	1708 vw, vvbr		1701 vw, vbr
C═O stretch out of phase (secondary amide)	1665 m	1669 m	1666 m
C═O stretch in phase (secondary amide)	1650 s	1650 m	1649 s
HOH deform	1638 m	1636 w	1635 w
Traces	1625 w		1622 w
C═O stretch out of phase (hydroxamate)	1586 m	1586 m	1586 m
C═O stretch in phase (hydroxamate)	1573 vs	1573 s	1573 s
NH_3^+ sym deform	1550 m, br	1545 m, br	1551 m
CH_2	1471 w	1472 m	1472 m
CH_3	1459 s	1461 m	1463 m
C–H vibrations: exact			1457 m
location derives from	1449 w	1450 w	1449 m
adjacency of different	1436 w	1438 w	1436 m
functional groups	1421 w	1421 m, br	1422 m
	1411 vw		1413 m
Traces			1396 vw
CH_3	1373	1373	1376 w, br
	1360	1363	1362 vw, br
			1351 m, br
C–N stretch N–H bend (secondary amide)[b]	1261	1260	1260
C–N stretch[b]	1181	1181	1181
	1139 w	1139 w	1139 w
N–O[b]	995	995	995
	980	980	980

[a] Relative band height (s, strong; m, medium; w, weak; v, very) and shape (sp, sharp; br, broad) are described. The shape of bands with an average broadness is not mentioned in the table. [b] These bands were determined without curve-fitting.

Curve-fitting of the ferrioxamine B spectrum (**Table 2**) revealed that absorption bands of both types of C═O (that of the secondary amide and the hydroxamate groups) were split upon iron chelation into two bands due to out-of-phase and in-phase vibrations (1665 and 1650 cm^{-1} and 1586 and 1573 cm^{-1}, respectively). Another striking effect of iron chelation at this range was the disappearance of the OH deformation band at 1396 cm^{-1} (**Figure 3B**). The CN−H stretching vibration, which splits into two bands at 1271 and 1254 cm^{-1} in the desferrioxamine B spectrum, shifted and merged at 1261 cm^{-1} in that of ferrioxamine B (**Figure 3B**). The band at 1163 cm^{-1} that was exhibited in the desferrioxamine B spectra (**Figure 3B**; **Table 1**), assigned to one type of CN vibration, disappeared in the spectra of ferrioxamine B (**Figure 3B**; **Table 2**). Small peaks in the range of NO at 950−990 cm^{-1} were shifted and elevated in the spectrum of ferrioxamine B compared to those bands in the spectra of desferrioxamine B.

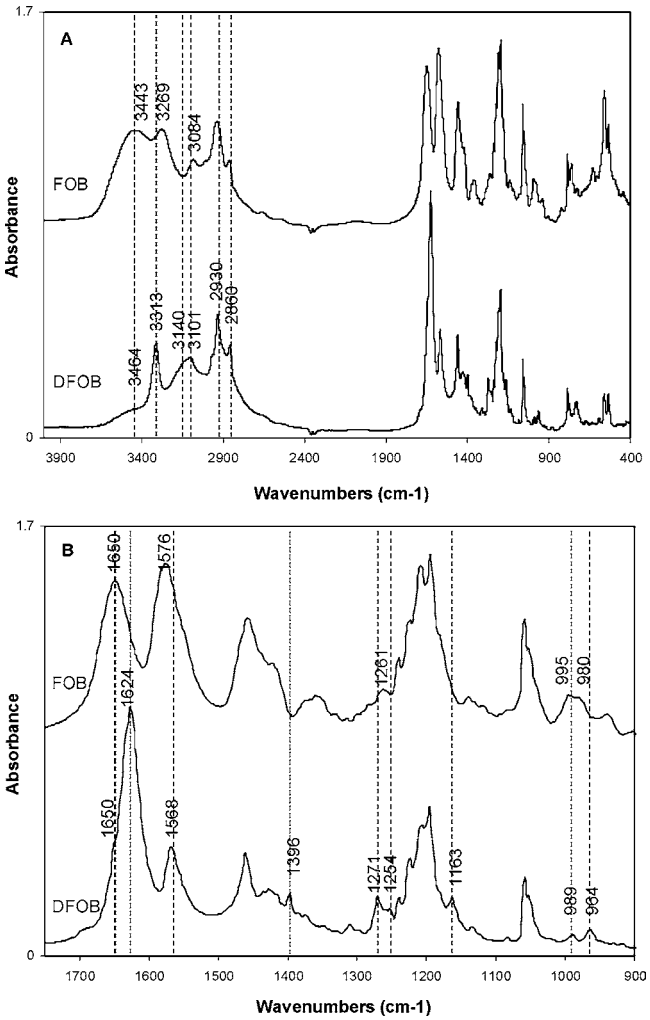

Figure 3. FTIR spectra of desferrioxamine B and ferrioxamine B recorded at 25 °C, pH 7.5. The KBr disks contained 0.5 and 2 mg of dry powder, respectively: (**A**) spectrum in the range of 4000–400 cm^{-1}; (**B**) magnification of the 1750–900 cm^{-1} range. Major peak wavenumbers are indicated. Dotted lines refer to major peaks in the desferrioxamine B spectrum, which are significantly affected by the Fe^{3+} chelation.

Thermal Treatments. The spectra following the 60 °C treatments exhibited intermediate trends of changes obtained by comparing the 25 °C treatments to those heated to 105 °C and were, therefore, omitted from the figures and tables to simplify the data presentation.

The most prominent effect of the thermal treatments of 60 and 105 °C on the higher range of the spectra was the elimination of water bands in the range of 3600−3350 cm^{-1} in the spectra of both desferrioxamine B (**Figure 4A**; **Table 1**) and ferrioxamine B (**Figure 5A**; **Table 2**) due to dehydration. Water bands in the lower frequency range of both desferrioxamine B and ferrioxamine B decreased as well, following the 105 °C thermal treatment (**Tables 1** and **2**). As a result, the shoulder at 1650 cm^{-1} in the desferrioxamine B spectra became more prominent (**Figure 4B**). Indeed, curve-fitting revealed that this band already existed in the spectra at 25 °C (**Table 1**) but was not observed due to overlapping with water bands.

A new peak evolved at 1700 cm^{-1} (**Figure 4B**; **Table 1**) in the spectrum of desferrioxamine B following the 105 °C

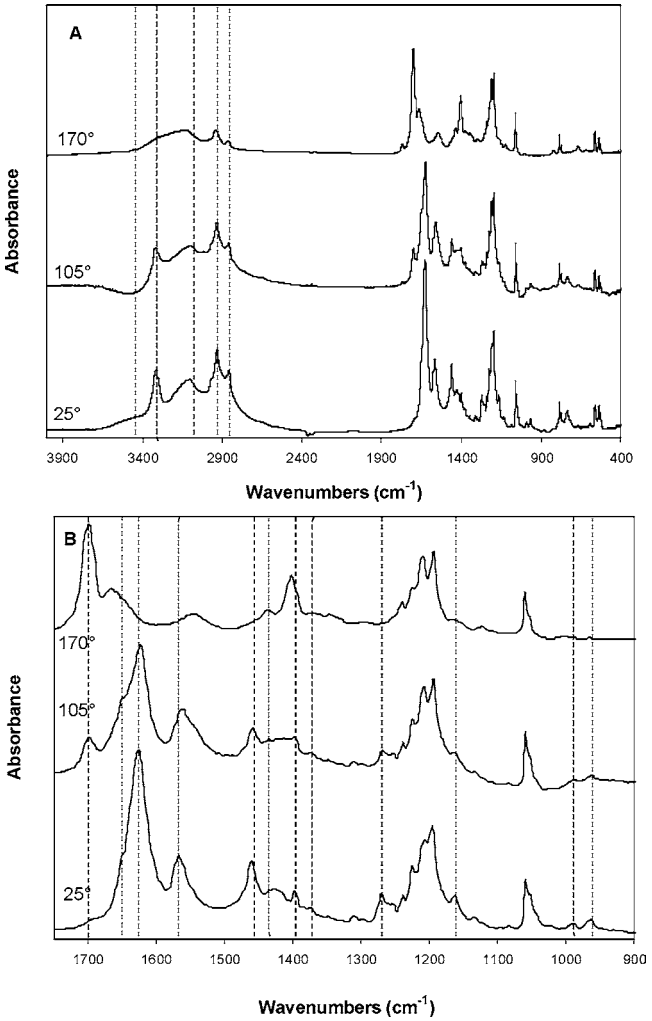

Figure 4. Effects of thermal treatments (25, 105,170 °C) on FTIR spectra of desferrioxamine B, obtained at pH 7.5. The KBr disks contained 0.5 mg of dry powder: (**A**) spectrum in the range of 4000–400 cm^{-1}; (**B**) magnification of the 1750–900 cm^{-1} range.

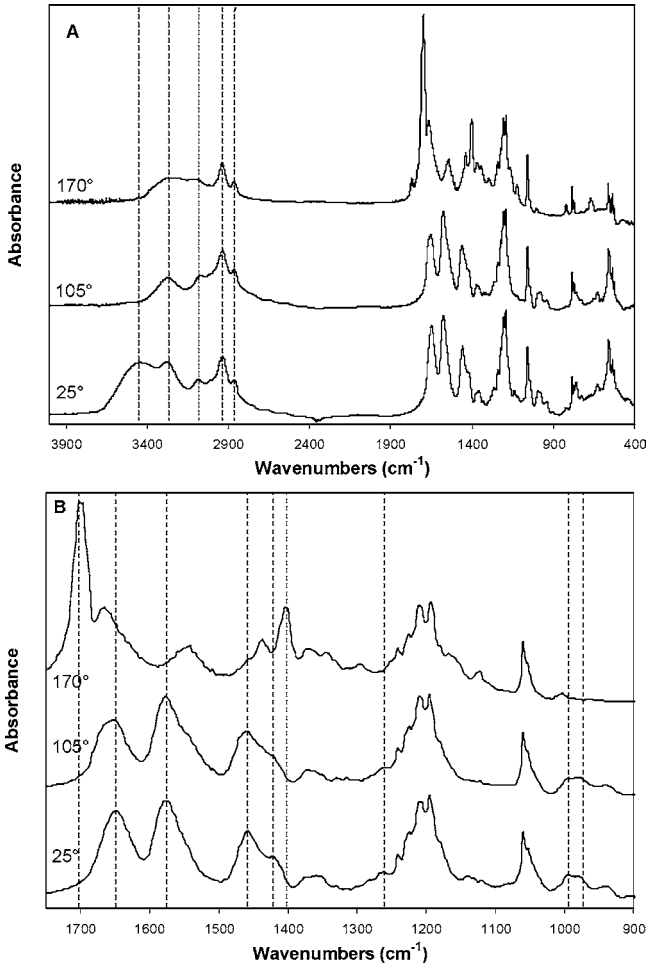

Figure 5. Effects of thermal treatments (25, 105, 170 °C) on FTIR spectra of ferrioxamine B, obtained at pH 7.5. The KBr disks contained 2 mg of dry powder: (**A**) spectrum in the range of 4000–400 cm^{-1}; (**B**) magnification of the 1750–900 cm^{-1} range.

treatment. This band had already appeared as a small shoulder at 25 and 60 °C. In contrast, in the ferrioxamine B spectra it was not evident even following the 105 °C treatment (**Figure 5B**; **Table 2**). However, shifts of the C−NH of the secondary amide and NH_3^+ absorption bands, resulting from these thermal treatments, were more significant for the ferrioxamine B spectra (**Tables 1** and **2**).

As opposed to the moderate effects, which resulted from the thermal treatments at 25, 60, and 105 °C, that of 170 °C caused an advanced level of destruction of the molecular structure. As a result, the structures of both desferrioxamine B and ferrioxamine B became very similar (**Figures 4** and **5**). The double peak of C−H at 2937 and 2862 cm^{-1} remained stable. The new peak that appeared in the spectrum of desferrioxamine B following the 105 °C treatment became very strong, followed by a peak of medium intensity at 1666 cm^{-1}. Typical peaks of the amide and hydroxamate groups disappeared. The shoulder at 1547 cm^{-1}, assigned to NH_3^+, which was better distinguished after the heating to 105 °C, remained as an individual peak in this region following the treatment of 170 °C. The peak at 1400 cm^{-1} was dramatically enhanced in the spectra of both desferrioxamine B and ferrioxamine B.

Effect of pH. In the lower range (4−7.5), the pH had no effect on either desferrioxamine B or ferrioxamine B (**Figures 6** and **7**, respectively). At pH 9 various changes appeared in the desferrioxamine B spectrum (**Figure 6**). The most striking ones were wide bands, which appeared in the range of 2600−2800 cm^{-1}; changes in the range 1700−1620 cm^{-1} resembling the effect of the 105 °C treatment (**Figure 8**) on the desferrioxamine B spectrum (appearance of new bands at 1699 and 1671 cm^{-1} and an emphasis of the shoulder at 1650 cm^{-1}); the peak at 1398 cm^{-1} and the area around it being significantly amplified; the peak at 1271 cm^{-1} declining and the range of 1010−960 cm^{-1} being elevated (**Figure 7**; **Table 1**). Small changes in the range of 700−910 cm^{-1} appeared in the desferrioxamine B spectrum at pH 9, as well as in that of ferrioxamine B (**Figures 6** and **7**). Curve-fitting analysis revealed a few more details upon comparison of desferrioxamine B spectra obtained at pH 7.5 and 9 (**Table 1**): peaks of NH_3^+ at 3000, 2903, 1607, and 1548 cm^{-1} were significantly decreased, and, instead, new peaks assigned to NH_2, appeared at 3323, 3410, and 1596 cm^{-1}.

DISCUSSION

The molecule of the siderophore ferrioxamine B contains several functional groups. The FTIR absorption bands of these groups overlap significantly, thus complicating the interpretation of the spectra. To overcome this complication, the spectra were curve-fitted. In the Results section we have described the effects of the various treatments (iron chelation, thermal treatments, and different pH conditions) on the spectra. The differential

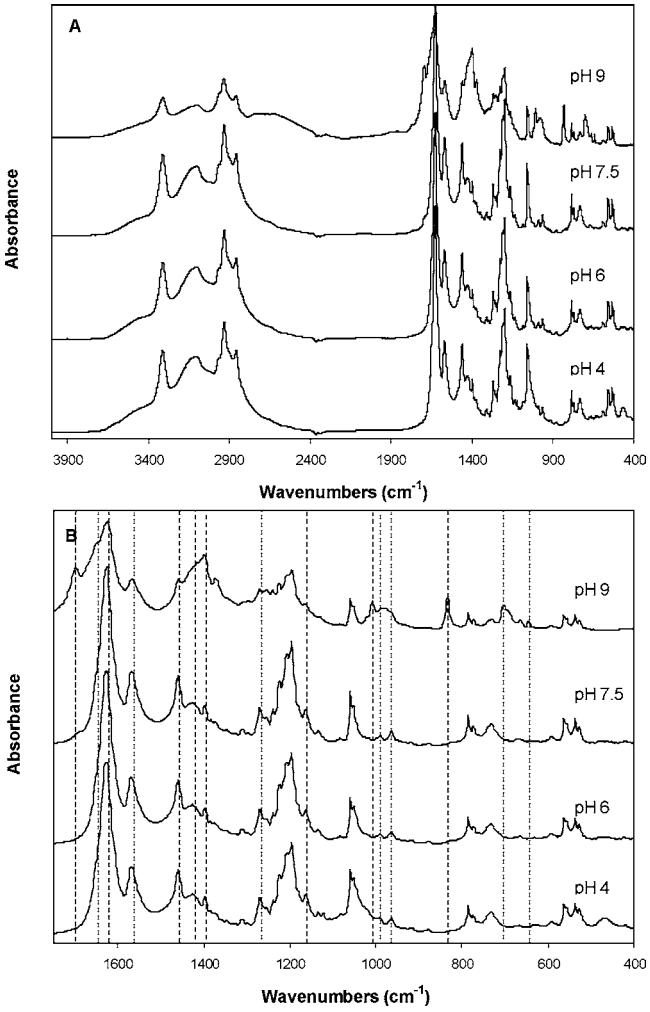

Figure 6. Effects of pH (4, 6, 7.5, 9, at 25 °C), on FTIR spectra of desferrioxamine B. The KBr disks contained 0.5 mg of dry powder: (**A**) spectrum in the range of 4000–400 cm^{-1}; (**B**) magnification of the 1750–400 cm^{-1} range.

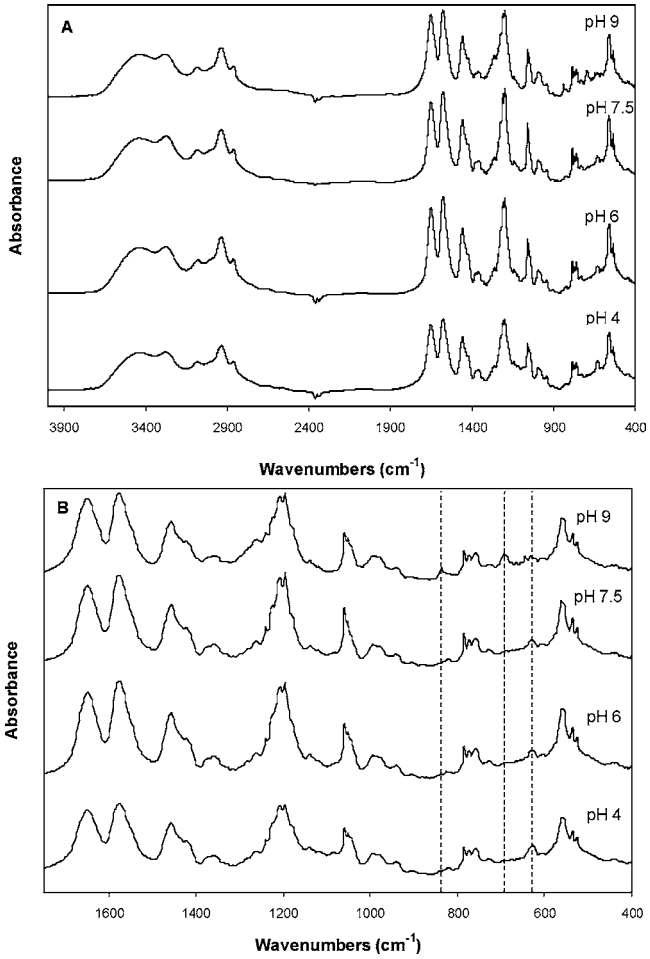

Figure 7. Effects of pH (4, 6, 7.5, 9, at 25 °C) on FTIR spectra of ferrioxamine B. The KBr disks contained 0.5 mg of dry powder: (**A**) spectrum in the range of 4000–400 cm^{-1}; (**B**) magnification of the 1750–400 cm^{-1} range.

reaction to these treatments enabled us to assign most of the peaks to the appropriate functional group. The following discussion refers to the spectrum of desferrioxamine B at 25 °C and pH 7.5, as a reference, and specifies the changes following the various treatments. The absorption intensities in the spectra of ferrioxamine B were lower, compared to those in the desferrioxamine B spectra (note the different concentrations of desferrioxamine B and ferrioxamine B in the KBr disks for the spectra presented in **Figure 3**), due to the restricted and rigid molecular conformation of the iron complex.

Secondary Amide [R−C(═O)−NH−R]. There are two secondary amide groups in the ferrioxamine molecule. They make up part of the residual chain of the hexadentate ligand, but they are not included in the chelation ring itself (**Figure 1**).

According to the literature, the amide−carbonyl stretching absorption (amide I band) is the broadest in the carbonyl family and is positioned between 1695 and 1615 cm^{-1}. In dry samples of secondary amides in an open chain, this bond absorbs at a wavenumber of ∼1640 cm^{-1} (*17*). We assigned the shoulder at 1650 cm^{-1}, which is fused into the stronger peak of the hydroxamate group at 1624 cm^{-1} and revealed upon dehydration (**Figure 4**), to that C═O bond. Upon Fe^{3+} chelation, the hydroxamate band shifts from 1624 cm^{-1} to a lower frequency, thus exposing the absorption band at 1649−1650 cm^{-1} in the ferrioxamine B spectra (**Figure 3**). This band was found to be very stable at all treatments (**Tables 1** and **2**). Due to the rigid structure formed by the iron chelation, the C═O vibration splits into two bands, in-phase and out-of-phase, in the ferrioxamine B spectrum; the first is at 1665 cm^{-1} and the other remains at 1650 cm^{-1} (**Table 2**).

Another strong band (amide II band) in the range of 1515−1570 cm^{-1} results from the NH bending vibration coupled with that of C−N stretching, when hydrogen is in the trans position to the carbonyl (*17*). At 25 °C this band appears in the spectrum of desferrioxamine B at 1568 cm^{-1} (**Figure 3**) and shifts upon dehydration to 1562 cm^{-1} (**Figure 4**). When the hydrogen of secondary amides is forced into the cis position, due to ring formation, this absorption is shifted to near 1430 cm^{-1} and the carbonyl absorbs strongly at 1695 cm^{-1} (*17*). This did not occur upon Fe^{3+} chelation, and thus it is assumed that the hydrogen remains at the trans position in the chelation ring. As no significant change is expected in this band upon iron chelation, the disappearance of the peak at ∼1560 cm^{-1} and the significant increase of the peak at 1576 cm^{-1} exhibited in the spectra of ferrioxamine B (**Figure 3**) were surprising. The shift of the C═O band of the hydroxamate group from 1624 to 1576 cm^{-1} due to iron chelation, which hides the amide II band around 1560 cm^{-1}, provides an explanation.

The curve-fitting work revealed that the C−NH bending vibration at 1568 cm^{-1} in the desferrioxamine B spectra splits into two peaks at 1571 and 1564 cm^{-1} (**Table 1**). The same interaction (C−N−H) should give rise to another small peak

in the range of 1275 ± 55 cm^{-1} (amide III), which is chiefly C−N stretching coupled with in-plane N−H bending (*18*, *19*). Indeed, two small peaks at 1271 and 1254 cm^{-1} appeared in the desferrioxamine B spectrum (**Figure 3b**; **Table 1**). This split could be attributed to the different strengths of the hydrogen bonds as suggested for the amide group of alachlor by Nasser et al. (*20*). We could not find a distinct band assigned to the C−N−H interaction in the range of 1590−1550 in the curve-fitting analysis for the ferrioxamine B spectra. It is assumed that this amide II band is completely hidden due to the overlap and similar shape of the peaks of the strongest C═O absorption bands. However, the aforementioned peaks, assigned as the amide III band of the secondary amide, merged into one peak at 1261 cm^{-1} in the ferrioxamine B spectrum (**Figure 3B**; **Table 2**). This result implies that the organized rigid structure of ferrioxamine B enables only one form of hydrogen bond with this group. This assumption is strengthened by the observation of other characteristic absorption bands of this group: secondary amides have a single N−H stretching vibration, which absorbs in the high wavenumbers range, at ∼3335 cm^{-1} (*17*). This is attributed to the sharp band, which appears in the desferrioxamine B spectra at 3313 cm^{-1} (**Figure 3A**; **Table 1**). In the ferrioxamine B spectra the frequency of this band significantly decreased to 3269 cm^{-1} (**Figure 3A**; **Table 2**). Because secondary amide groups do not participate in the formation of the chelation ring itself, this effect can be attributed only to changes in its proximal environment. The significant shift and broadness of the peak at 3269 cm^{-1} imply that very specific hydrogen bonds were taking place. We believe that the fixed spatial structure of ferrioxamine B facilitates the formation of highly specific intramolecular bonds. A hydrogen bond between the N-H of the secondary amide and the C═O of the hydroxamate is proposed as a reasonable site for this interaction based on steric considerations. An overtone of the C−N−H interaction of the secondary amide group should appear at ∼3075 cm^{-1} (*17*). This band is attributed to a peak at 3096 cm^{-1} in desferrioxamine B (**Figure 2**; **Table 1**) and shifts, here as well, to 3084 cm^{-1} in the ferrioxamine B spectrum (**Table 2**). The frequency of the latter decreased to 3071 cm^{-1} following heating in the 105 °C treatment, implying that water reduced the strength of the abovementioned specific hydrogen bond. The secondary amide group was not significantly affected by pH in the examined range.

Hydroxamate Group −[R−C(═O)−N(OH)−R]. The ferrioxamine molecule contains three hydroxamate groups. Upon deprotonation of the hydroxyls, the molecule becomes a hexadentate ligand highly specific for Fe^{3+}. The Fe^{3+} binds to both oxygen atoms of each hydroxamate group (*21*, *22*), creating a distorted octahedron (*12*). The absorption band of the carbonyl in tertiary amides appears in the range of 1665−1640 cm^{-1} and is sharper and stronger than that of secondary amides (*17*). Studies of hydroxamic acids found the strong carbonyl absorption in the wider range of 1700−1595 cm^{-1} (*15*). Indeed, the sharp and very strong absorption of the hydroxamic C═O appeared at 1624 cm^{-1} in the desferrioxamine B spectrum (**Figure 3**; **Table 1**).

The Fe^{3+} is bound to the desferrioxamine B molecule via the two oxygen atoms of each hydroxamate group, releasing the hydroxyl H^+. Thus, we expected the disappearance of the OH band due to deprotonation, as well as changes in the C═O, C−N, and N−O absorption bands. As a result of the resonance in the chelation ring, the absorption of C═O is expected to decrease significantly due to the rise in its single bond (C−O) character. Indeed, studies of FTIR spectra of hydroxamic acids have shown broadening of the bands of the C═O vibration and a frequency decrease of 40−60 cm^{-1} upon chelation of Fe^{3+} (*16*, *23*). X-ray crystallography of solid siderophores has also shown a decrease in the distance of C to N and an increase in C═O distance following iron complexation (*24*−*28*). The same effect has been proposed for the ferrioxamine B structure (*12*), but the C to N distance of the hydroxamic group in the free ligand (desferrioxamine B) has not been measured yet. The results of our study support this assumption. Indeed, the frequency of the C═O absorption decreased significantly from 1624 cm^{-1} in the desferrioxamine B spectrum to 1586 and 1573 cm^{-1} in the ferrioxamine B spectrum, and its intensity was lower (**Table 2**). Here, as well as for the amide group, the C═O vibration splits into two bands due to the rigid structure of the complex with iron.

Due to the resonance assumption, the appropriate C−N absorption frequency was supposed to increase significantly according to a rise in its double-bond character (C═N). Absorption of the C−N bond in amides as well as amines groups usually appears in the range of 1175−1055 cm^{-1} (*17*). Three peaks were evident in this range in the spectra of desferrioxamine B at 1134, 1163, and 1181 cm^{-1}. Upon Fe^{3+} chelation, the band at 1163 cm^{-1} disappeared (**Figure 3**; **Tables 1** and **2**). We believe that the frequency of this vibration increased due to the resonance in the chelation ring. Its new location may be hidden by the strong absorption of the SO_3 group. The intensification of the resonant form following Fe^{3+} chelation is significant for the function of the siderophore, because it enlarges the negative charge on the carbonylic oxygen, thus strengthening the metal binding.

The (N)−OH stretching band in oximes absorbs in the range of 3450−3030 cm^{-1} (*17*). This vibration was attributed to the wide conspicuous band, which appeared at 3149 cm^{-1} in the desferrioxamine B spectrum (**Table 1**). It was found to be very sensitive to the environmental conditions as revealed by the effects of the different pH levels and thermal treatments, due to the reactionary character of the OH group. This band is absent in the spectrum of ferrioxamine B due to its deprotonation. Absorption of the bending vibration of the (N)−OH group is expected in the range of 1420−1330 cm^{-1} (*18*). Disappearance of the peak at 1396 cm^{-1} from the spectrum of ferrioxamine B (**Figure 3**; **Tables 1** and **2**) suggests its assignment to the (N)−O−H bending vibration. The N-O stretching vibration in oximes gives rise to a strong absorption band at 1055−870 cm^{-1}. This peak splits at times into several bands (*17*). Earlier studies of hydroxamic acids found this band at 965 and 990−1000 cm^{-1} (*15*, *16*). Only weak absorption bands were shown at this range in our spectra, implying that the absorption was indeed split into two peaks at 989 and 964 cm^{-1} in the desferrioxamine B spectrum (**Figure 3**; **Table 1**). The N−O bond is expected to strengthen upon iron chelation, and thus this vibration is expected to intensify and its frequency to increase. Indeed, peak frequency and intensity were enhanced and appeared in the ferrioxamine B spectra at 995 and 980 cm^{-1} (**Figure 3**; **Table 2**). The same increase in NO frequencies was found in studies of FTIR spectra of hydroxamic acids (*16*, *23*).

A medium-strong peak evolved at 1700 cm^{-1} following treatments at 105 °C as well as at pH 9 (**Figure 8**). In the latter (pH 9), this effect was more drastic; it was accompanied by another new peak at 1671 cm^{-1} and an evident weakening of the intensity of the hydroxamic carbonyl peak (1624−1622 cm^{-1}) compared to that of the secondary amide carbonyl at 1650 cm^{-1}. The peak at 1700 cm^{-1} became very strong, for both desferrioxamine B and ferrioxamine B, at 170 °C, as did the

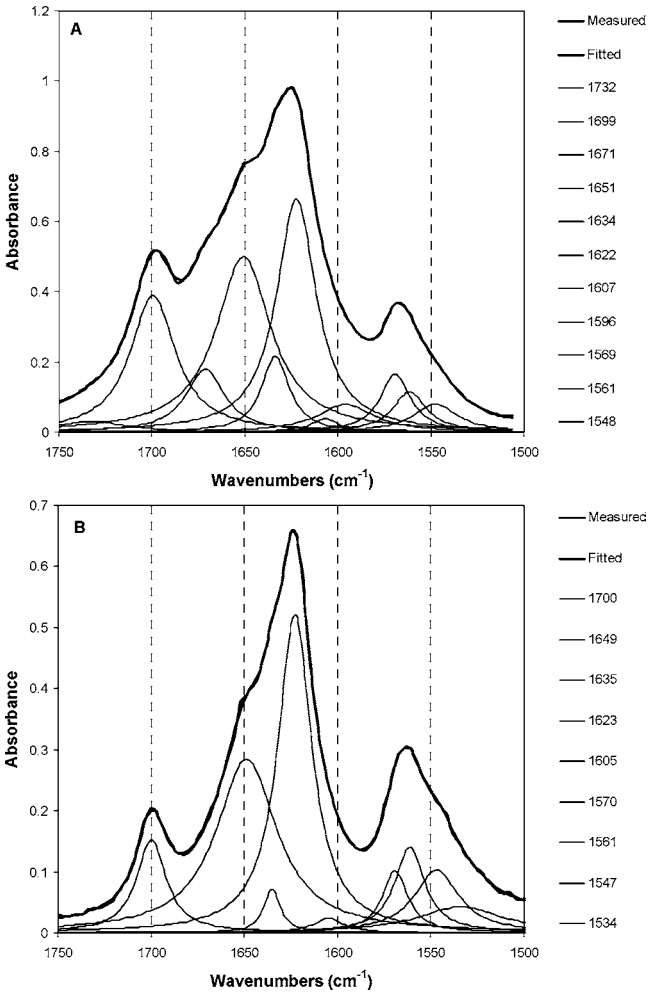

Figure 8. Curve-fitted spectra of desferrioxamine B (0.5 mg) recorded in KBr disks: (**A**) obtained at pH 9.0, 25 °C; (**B**) obtained at pH 7.5, after heating to 105 °C. Bold lines represent measured spectrum and fitted line, which are overlapping. Gray lines represent the spectra assembling the fitted line as it was analyzed using GRAMS/AI software produced by Thermo Galactic. Peak values are listed on the right.

medium peak at 1666 cm^{-1} (**Figures 4B** and **5B**). Because the 170 °C treatment caused complete destruction of hydroxamic and amide groups, it is suggested that the new peaks, which appeared in the 105 °C and pH 9 treatments, represent partial degradation of the desferrioxamine B molecule under these conditions. Changes were also observed in the region between 1460 and 1375 cm^{-1} in the spectrum of desferrioxamine B at pH 9 (**Figure 7B**). Because the exact location of C−H absorption bands in this region depends on their chemical environment (*29*), the changes exhibited in this range in the spectrum of desferrioxamine B at these conditions are in accordance with the degradation of certain functional groups. The hydroxamic carbonyl appeared to be more sensitive to high levels of temperature and pH. A lack of a proton donor in both treatments (due to dehydration and alkaline conditions, respectively) may be a catalyzing factor for this process.

The OH deformation band at 1397 cm^{-1} is enhanced at pH 9 as well (**Figure 7**). The intensity of the OH stretching band was not reduced, although it shifted to a lower frequency, implying stronger hydrogen bonds. Therefore, we concluded that the OH groups do not yet undergo deprotonation at pH 9. The intensity of the N−O stretch vibration was strengthened at pH 9, and a new band appeared in its region at 1009 cm^{-1} (**Figure 7**; **Table 1**), probably due to the effect on the adjacent C═O group.

NH_3^+ Group. The NH_3^+ group is the most difficult to identify unequivocally in the FTIR spectrum of ferrioxamine B. This group exhibits a strong and broad absorption band in the range of 2800−3000 cm^{-1}, frequently termed the "ammonium band". This band consists of symmetric and asymmetric stretching vibrations (*18*, *29*). According to other researchers it can reach 3200 cm^{-1} (*30*). It is accompanied by overtones and combination tones at 2800−2000 cm^{-1}. The ammonium band overlaps with the strong CH absorption bands, and thus it cannot be completely recognized in the spectra of desferrioxamine B and ferrioxamine B. Using curve-fitting, its bands were recognized at 3013 and 2901 cm^{-1} in the desferrioxamine B spectrum and at 3012 and 2947 cm^{-1} in the ferrioxamine B spectrum. The different locations of ammonium bands imply stronger hydrogen bonds of this group with exposed functional groups along the linear molecule of desferrioxamine B compared to those in the ferrioxamine B molecule. At the latter, these functional groups are gathered around the iron center, creating strong intramolecular bonds, whereas the NH_3^+ at the end of the pendant tail remains out of this compact structure. Thus, bonds through the free terminal NH_3^+ with the rather hydrophobic outer face are less intensive. Due to the high reactivity of NH_3^+, it is very sensitive to environmental conditions. Its absorption may change significantly according to the water content of the sample, pH, and adjacent functional groups. These effects were more prominent in the spectra of ferrioxamine B (**Table 2**) than in those of desferrioxamine B (**Table 1**). Here, as well, the difference could be related to the strong bonds formed by NH_3^+ with other functional groups in the desferrioxamine B molecules compared to that group in ferrioxamine B molecules, which mainly reacts with the solution components.

Symmetric and asymmetric bending vibrations of NH_3^+ are usually exhibited in the region of 1575−1600 cm^{-1} as well as 1500−1550 cm^{-1} (*18*, *29*). In some instances, only one band appears (*30*). A broad peak, which appeared in the desferrioxamine B spectrum at 1608 cm^{-1} (**Table 1**), was assigned to this group. A relatively broad band observed at 1550 cm^{-1} was related to the NH_3^+ group as well. At pH 9, absorption intensities of the NH_3^+ stretching vibrations at 3013 and 2901 cm^{-1} in the spectrum of desferrioxamine B were reduced and new bands appeared at 3410 and 3323 cm^{-1}. These bands are characteristic of the NH_2 (*29*) formed due to deprotonation of NH_3^+. The peak at 1608 cm^{-1} was also reduced, whereas a new one appeared at 1596 cm^{-1}, implying the appearance of NH_2. A decrease in absorption of this group at pH 9 was observed only in the desferrioxamine B spectrum, whereas the ferrioxamine B spectrum remained unchanged. This observation is in accordance with their protonation constants at 8.3 and 10.4, respectively (*11*). These results indicate that the deprotonation of desferrioxamine B begins with the NH_3^+ group. The state of the NH_3^+ group is expected to be significant to the siderophore function because the cationic tail may play an important role in the recognition of ferrioxamine B by its host membrane receptors, as suggested by some researchers (e.g., refs *31* and *32*).

C−H Interactions. Bands of the aliphatic chains were relatively stable under all examined conditions in both desferrioxamine B and ferrioxamine B spectra. The most striking bands of these bonds were CH_2 observed via a typical double peak resulting from a symmetrical and nonsymmetrical stretching of methylene at about 2930 and 2860 cm^{-1}. CH_3 absorption is responsible for the weaker shoulders exhibited by curve-fitting

as smaller peaks around 2960 and 2870 cm^{-1} (**Figure 2**; **Tables 1** and **2**). In contrast to the other stretching vibrations of CH, the asymmetric peak of CH_3 changed upon Fe chelation and in relation to water content (**Table 2**). This reaction is in accordance with its adjacency to the hydroxamate group (**Figure 1**). A series of peaks, which appeared in the range of 1470−1406 cm^{-1} (**Tables 1** and **2**) were attributed to different CH vibrations derived from the proximity of different functional groups. The enhanced peak at ∼1460 cm^{-1} was attributed to CH_3 attached to the C═O group (*29*). This association with the Fe-binding center is the reason for the relatively large difference in this region between the desferrioxamine B and ferrioxamine B spectra.

Water in the Sample. Water peaks are prominent in the higher wavenumber range. In the desferrioxamine B spectra, they appear as a single broad band at 3464 cm^{-1} (**Figure 2**; **Table 1**), which disappear upon thermal dehydration. In the ferrioxamine B spectrum the appearance of the water bands was completely different. A series of medium-to-strong bands revealed by the curve-fitting analysis at 3600−3350 cm^{-1} (**Table 1**) creates a strong broad band in the spectrum of ferrioxamine B (**Figure 3A**). It seems that the ferrioxamine B molecule, having a compact and rigid structure, binds the water molecules in a more structured manner than that of the linear and polar molecule of desferrioxamine B.

Absorption bands of both the C−N−H overtone of the amide group and the NH_3^+ symmetric stretching were significantly affected in the ferrioxamine B spectra by water dehydration, indicating that hydrogen bonds were strengthened by the loss of water. The possible role of water in the stabilization of the molecular structure needs a further examination, as previously discussed. In the lower range, the water band at 1635 cm^{-1} also decreased significantly upon thermal dehydration (**Tables 1** and **2**). According to this band, water loss is more drastic from desferrioxamine B than from ferrioxamine B.

Sulfonic Group ($CH_3SO_3^-$). The sulfonic group is not an integral part of the molecule, but rather a counteranion to the desferrioxamine B cation, and exhibited prominent bands series in all of the spectra shown in this work. The peak series that begins at 1240 cm^{-1} and reaches its peak at 1195 cm^{-1} belongs to this group. Another significant band was exhibited by this group at ∼1058−1053 cm^{-1} (**Figure 3**).

Thermal Treatment at 170 °C. As opposed to the minor effects of the 25−105 °C thermal treatments, that of 170 °C resulted in a decomposition of the molecular structures of both desferrioxamine B and ferrioxamine B (**Figures 4** and **5**). The resemblance between the products of the decomposition for both molecules implies the loss of the iron center, which stabilizes the structure of the iron complex and disintegration of the same bonds in both instances, rather than an accidental disruption. The changes, which took place upon heating, were very helpful in our effort to achieve definitive peak assignments. Peaks involved in the C−N−H bond of the secondary amide, such as at 3311, 1568, and 1271 cm^{-1} in the desferrioxamine B spectrum (**Figure 4**) and at 1560 and 1261 cm^{-1} in that of ferrioxamine B (**Figure 5**), disappeared after heating to 170 °C. The same occurred for the strong peak of the hydroxamic group at 1624 cm^{-1} in the desferrioxamine B spectrum and at 1586 and 1573 cm^{-1} in that of ferrioxamine B. Bands in the C−N and N−O region were reduced significantly or disappeared. As already mentioned, a very strong peak appeared in the spectra of desferrioxamine B and ferrioxamine B, following heating to 170 °C, at 1700 cm^{-1} followed by another significant peak at 1666 cm^{-1}. According to its location, the peak at 1700 cm^{-1} probably results from the C═O bond, indicating that coupling between the carbonyl and nitrogen in the hydroxamate and amide groups was interrupted. A strong band in the O−H bending region near 1400 cm^{-1} may indicate enhancement of the hydroxyl absorption due to detachment from the carbonyl of the hydroxamate group. However, because the N−O absorption changed significantly or vanished under these conditions, it is hard to determine whether the 1400 cm^{-1} band results from the N−OH vibration or is a product of a molecular disintegration. Bands of the C−H stretching were retained in the spectra of this treatment, but the bending bands in the lower range (1470−1406 cm^{-1}), which derived from an association with different functional groups, were partially impaired. This change was most prominent for the strong CH_3 peak at ∼1460 cm^{-1}, which was significantly affected upon heating to 170 °C due to its association with the hydroxamate group. From the existence of the characteristic broad absorption at 3018 and 1545 cm^{-1}, it appears that the NH_3^+ group was not impaired.

Summary. The goal of this study was to elaborate the FTIR spectra of the siderophore ferrioxamine B, in its free and iron-bound configurations, to develop an easy tool for diagnosing the state of these molecules. A comparison of the results of the various pH and heating treatments enabled us to assign most of the significant bands to the appropriate vibrations. Identification of some characteristic absorption bands, especially those of NH_3^+, required the use of curve-fitting analysis. The full clarification of the FTIR spectra of the desferrioxamine B and ferrioxamine B molecules achieved in this study provides crucial information on the condition of each functional group. Our data facilitate the distinction between the free ligand and the iron complex. Using the analysis of the FTIR spectra we have found various characteristics of a highly stabilized molecular structure of the ferric complex of the siderophore. These characteristics are useful for the study of different environmental conditions' impact, as well as interactions with other materials, on the stability of the iron−siderophore complex. Changes in the conformation of the ferric complex and the pendent tail with the terminal NH_3^+ can affect the ability of microorganisms and plants to use the siderophore as an iron source. The interaction of the functional groups in the open chain of the free ligand could significantly influence its ability to bind the metal and create a stable complex. All of these aspects can be analyzed in detail using FTIR spectra and their proposed interpretation. High levels of pH and temperature caused a partial decomposition of the desferrioxamine B molecule and especially of the hydroxamic groups, which hold the iron in the ferric complex. These effects have to be considered in further investigation and potential utilization of the siderophore. The FTIR analyses proposed provide an attractive tool for studying the siderophore behavior in neutral environments.

LITERATURE CITED

(1) Chen, Y.; Barak, P. Iron nutrition of plants in calcareous soils. *Adv. Agron.* **1982**, *35*, 217−240.

(2) Chen, Y.; Shenker, M. Agronomic approaches for increasing iron availability to food crops. Agricultural and molecular genetic approaches to improving nutrition and preventing micronutrient malnutrition globally. In *Encyclopedia of Life Support Systems (eolss)*; developed under the auspices of UNESCO; Cakmak, I., Graham, R. D., Welch, R. M., Eds.; EOLSS: Oxford, U.K., 2003.

(3) Lindsay, W. L. *Chemical Equilibria in Soils*; Wiley: New York, 1979.

(4) Winkelmann, G. Specificity of iron transport in bacteria and fungi. In *CRC Handbook of Microbial Iron Chelates*; Winkelmann, G., Ed.; CRC Press: Boca Raton, FL, 1991.
(5) Cline, G. R.; Reid, C. P. P.; Powell, P. E.; Szaniszlo, P. J. Effects of hydroxamate siderophore on iron absorption by sunflower and sorghum. *Plant Physiol*. **1984**, *76*, 36−39.
(6) Jurkevitch, E.; Hadar Y.; Chen, Y. Involvement of bacterial siderophores in the remedy of lime-induced chlorosis in peanut. *Soil Sci. Soc. Am. J.* **1988**, *52*, 1032−1037.
(7) Crowley, D. E.; Wang, Y. C.; Reid, C. P. P.; Szaniszlo, P. J. Mechanisms of iron acquisition from siderophores by microorganisms and plants. *Plant Soil* **1991**, *130*, 179−198.
(8) Wang, Y.; Brown, H. N.; Crowley, D. E.; Szaniszlo, P. J. Evidence for direct utilization of a siderophore, ferrioxamine B, in axenically grown cucumber. *Plant Physiol*. **1993**, *16*, 579−585.
(9) Siebner-Freibach, H.; Hadar, Y.; Chen, Y. Siderophores sorbed on ca-montmorillonite as an iron source for plants. *Plant Soil* **2003**, *251*, 115−124.
(10) Leong, J.; Raymond, K. N. Coordination isomers of biological iron transport compounds. IV: Geometrical isomers of chromic desferrioxamine B. *J. Am. Chem. Soc.* **1975**, *97*, 293−296.
(11) Martell, A. E.; Smith, R. M.; Motekaitis, R. J. *NIST Critically Selected Stability Constants of Metal Complexes Database (v. 4). Standard Reference Data Program*; NIST: Gaithersburg, MD, 1997.
(12) Dhungana, S.; White, P. S.; Crumbliss, A. L. Crystal structure of ferrioxamine B: A comparative analysis and implications for molecular recognition. *J. Biol. Inorg. Chem.* **2001**, *6*, 810−818.
(13) Bickel, H.; Bosshardt, R.; Gaumann, E.; Reusser, P.; Vischer, E.; Voser, W.; Wettstein, A.; Zahner H. Uber die isolierung und charakterisierung der ferrioxamine A−F, neuer wuchsstoffe der sideramin-gruppe. *Helv. Chim. Acta* **1960**, *43*, 2119−2128.
(14) Beyer, W. F.; Fridovich, I. Characterization of a superoxide-dismutase mimic prepared from desferrioxamine and MnO_2. *Arch. Biochem. Biophys*. **1989**, *271*, 149−156.
(15) Hadzi, D.; Prevorsek, D. Infra-red absorption bands associated with the nh group - iii. *Spectrochim. Acta* **1957**, *10*, 38−51.
(16) Holmen, B. A.; Tejedortejedor, M. I.; Casey, W. H. Hydroxamate complexes in solution and at the goethite-water interface: A cylindrical internal reflection Fourier transform infrared spectroscopy study. *Langmuir* **1997**, *13*, 2197−2206.
(17) Pouchert, C. J. *The Aldrich Library of Infrared Spectra*; Aldrich Chemical Co.: Milwaukee, WI, 1981.
(18) Silverstein, R. M.; Bassler, G. C.; Morrill, T. C. *Spectrometric Identification of Organic Compounds*, 5th ed.; Wiley: New York, 1991.
(19) Roeges, N. P. G. *A Guide to the Complete Interpretation of Infrared Spectra of Organic Structures*; Wiley: Chichester, U.K., 1994.
(20) Nasser, A.; Gal, M.; Gerstl, Z.; Mingelgrin, U.; Yariv, S. Adsorption of alachlor by montmorillonites. *J. Thermal Anal*. **1997**, *50*, 257−268.
(21) van der Helm, D.; Jalal, M. A. F.; Hossain, M. B. The crystal structures, conformations and configurations of siderophores. In *Iron Transport in Microbes, Plants and Animals*; Winkelmann, G., van der Helm, D., Neilands, J. B., Eds.; VCH: Weinheim, Germany, 1987; pp 135−165.
(22) Boukhalfa, H.; Crumbliss, A. L. Chemical aspects of siderophore mediated iron transport. *Biometals* **2002**, *15*, 325−339.
(23) Brown, D. A.; Mckeith, D.; Glass, W. K. Transition-metal complexes of monohydroxamic acids. *Inorg. Chim. Acta* **1979**, *35*, 5−10.
(24) van der Helm, D.; Poling, M. Crystal-structure of ferrioxamine-e. *J. Am. Chem. Soc*. **1976**, *98*, 82−86.
(25) Hossain, M. B.; van der Helm, D.; Poling, M. The structure of deferriferrioxamine e (nocardamin), a cyclic trihydroxamate. *Acta Crystallogr. Sect. B: Struct. Sci*. **1983**, *39*, 258−263.
(26) Mocherla, R. R.; Powell, D. R.; Barnes, C. L.; van der Helm, D. Structures of *N*-(4-cyanophenyl)acetohydroxamic acid, $C_9H_8N_2O_2$ (i), and tris[*N*-(4-cyanophenyl)acetohydroxamato]iron-(III) hydrate, $[Fe(C_9H_7N_2O_2)_3]\cdot 0.1H_2O$ (ii). *Acta Crystallogr. Sect. C: Crystal Struct. Commun*. **1983**, *39*, 868−871.
(27) Dietrich, A.; Powell, D. R.; Engwilmot, D. L.; Hossain, M. B.; van der Helm, D. Structures of 2 isomeric hydroxamic acids—*N*-methyl-*p*-toluohydroxamic acid (mth) and *N*-(4-methylphenyl)-acetohydroxamic acid (mpa). *Acta Crystallogr. Sect. C: Crystal Struct. Commun*. **1990**, *46*, 816−821.
(28) Dietrich, A.; Fidelis, K. A.; Powell, D. R.; van der Helm, D.; Engwilmot, D. L. Crystal-structures of tris *N*-(4-methylphenyl)-acetohydroxamato iron(iii)−acetone (1/1) and tris(*N*-methyl-4-methylbenzohydroxamato)iron(iii) and gallium(iii)−acetone−water (1/1/1)—structure−stability relationships for the hydroxamate complexes of Fe^{3+} and ga^{3+}. *J. Chem. Soc., Dalton Trans*. **1991**, 231−239.
(29) Nakanishi, K.; Solomon, P. H. *Infrared Absorption Spectroscopy*; Holden-Day: Oakland, CA, 1977.
(30) Yariv, S. IR spectroscopy and thermo-ir spectroscopy in the study of the fine structure of organo-clay complexes. In *Organo-clay Complexes and Interactions*; Yariv, S., Cross, H., Eds.; Dekker: New York, 2001.
(31) Spasojevic, I.; Crumbliss, A. L. Bulk liquid membrane transport of ferrioxamine B by neutral and ionizable carriers. *J. Chem. Soc., Dalton Trans*. **1998**, *23*, 4021−4027.
(32) Ziv, C. Characterization of structure−function relationship of iron uptake by microorganisms: The use of biomimetric synthetic analogs of ferrioxamine B. M.A. thesis, The Hebrew University of Jerusalem, Rehovot, Israel (Hebrew, with an English abstract), 2000.

Received for review October 1, 2004. Revised manuscript received December 29, 2004. Accepted December 31, 2004.

JF048359K